applied optics

Method for absolute measurement of flat surface

Lisong Yan,[1] Fazhi Li,[2] Xiaokun Wang,[3] Haidong Zhang,[3] Lei Zhang,[4] and Donglin Ma[1,*]

[1]School of Optical and Electronic Information and Wuhan National Laboratory for Optoelectronics, Huazhong University of Science and Technology, Wuhan 430074, China
[2]Hunan University of Technology, Zhuzhou, Hunan 412007, China
[3]Key Laboratory of Optical System Advanced Manufacturing Technology, Changchun Institute of Optics, Fine Mechanics and Physics, Chinese Academy of Sciences, Changchun 130033, China
[4]Key Laboratory of Opto-Electronic Information Acquisition and Manipulation, Ministry of Education, Anhui University, Hefei 230601, China
*Corresponding author: madonglin@hust.edu.cn

Received 20 July 2020; revised 29 October 2020; accepted 30 October 2020; posted 3 November 2020 (Doc. ID 403268); published 20 November 2020

Interferometry is a relative measurement method for optical surface testing, and thus its testing accuracy depends on the accuracy of the reference surface. Absolute measurement is one of the most effective methods to improve the testing accuracy in interferometry. We present an efficient absolute measurement method based on Zernike polynomial fitting algorithms. With our proposed method, the profiles of both the test surface and the reference surface can be calculated simultaneously. We further carried out simulation analysis to scientifically evaluate the test accuracy of the proposed method. Finally, we conducted actual experiments to demonstrate the feasibility and practicability of our method.

https://doi.org/10.1364/AO.403268

1. INTRODUCTION

Interferometry is widely used in optical surface testing. It can accurately measure the difference between the reference surface and the testing surface. In general, the precision of interferometry is limited by the accuracy of the reference surface. If the reference surface can be considered as a perfect one or is accurately known in advance, then the testing surface can be determined with a relatively high precision. However, both the reference surface and the testing surface are unknown in actual testing. As a result, if we want to improve the testing accuracy to the level of nanometer or sub-nanometer in interferometry, we should instead conduct absolute measurement, where the surface errors of the reference surface can be excluded.

The earliest absolute measurement method can be traced to the use of a liquid surface that has the same radius of curvature as the earth to serve as an ideal reference flat surface [1,2]. However, the instability problem associated with the liquid itself and the static electricity charge problem that perturbs the shape of the liquid surface make the method difficult to apply in actual flat surface testing. Then, the traditional three-flat method was proposed [3], and its related modified methods were studied by scholars [4–9]. In all of these three-flat methods, three reference surfaces are needed and complex procedures are necessary in testing. Keenan proposed a differential method [10], which was then extended and improved by Bloemhof [11], Ma *et al.* [12], and Huang *et al.* [13]. To accomplish the absolute testing of a 1.6 m diameter flat surface, Su *et al.* proposed a maximum likelihood method [14]. Combined with a 1 m reference surface and the stitching testing method, the flat mirror was measured with accuracy up to 2 nm [14]. Su *et al.* provided a shift-rotation absolute method to test a flat surface [15], and Yan *et al.* applied an orthonormal polynomial fitting absolute method to test the tertiary mirror at the Thirty Meter Telescope [16]. Aiming to solve the absolute testing of a high-numerical-aperture spherical surface, Yang *et al.* provided a high-order shift-rotation absolute measurement method [17,18].

In this paper, we propose an efficient absolute measurement method based on Zernike polynomial fitting algorithms. Our proposed method can reconstruct both the reference surface and the test surface simultaneously. In a situation where the reference surface error cannot be ignored, our proposed method can accomplish absolute testing with high accuracy. To demonstrate the performance of our absolute measurement method, both simulation and experiment are carried out. The paper is organized as follows. In Section 2, the basic theory of our proposed absolute measurement method is introduced. In Section 3, we conduct a simulation based on our proposed method to show the surface reconstruction accuracy of the algorithm. In Section 4, the actual experiment and the relative testing results are provided to demonstrate the feasibility and practicability of our method. The conclusion is given in Section 5.

2. THEORY

The testing surface can be described as a sum of Zernike polynomials in its domain as shown in Eq. (1). And the reference surface can also be expressed as a sum of Zernike polynomials in its domain as shown in Eq. (2). As both the reference surface and the test surface are usually described with discrete pixel points in domain areas, a kind of orthonormal Zernike polynomial is applied in the actual surface error description [19,20]:

$$W_t \approx \sum_{i=1}^{k} a_i Z_i, \tag{1}$$

$$W_r \approx \sum_{i=1}^{m} b_i Z_i'. \tag{2}$$

In Eqs. (1) and (2), W_t and W_r represent the test surface and the reference surface, respectively; a_i and b_i represent the relative Zernike coefficients; k and m represent the number of Zernike terms chosen to describe the test surface and the reference surface, respectively; and Z_i and Z_i' represent the ith Zernike polynomial term over the test surface and the reference surface, respectively.

Then a measurement result can be expressed as in Eq. (3):

$$\begin{aligned} D_1 = D_1' + \text{residuals} &= a_{11}Z_1(x,y) + a_{12}Z_2(x,y) \\ &+ a_{13}Z_3(x,y) + a_{14}Z_4(x,y) - \sum_{i=5}^{k} a_i Z_i(x,y) \\ &+ \sum_{i=5}^{m} b_i Z_i'(x',y') + \text{residuals}, \end{aligned} \tag{3}$$

where D_1 is the map of first interferometry; D_1' is the part of data that can be described analytically by Zernike polynomials; residuals is the part of the map that cannot be described by Zernike polynomials; a_{11}, a_{12}, a_{13}, and a_{14} represent the relative piston, tip, tilt, and defocus in the map of first interferometry; x and y are global coordinates of the testing surface; and x' and y' are the coordinates of the reference surface.

When there are translations dx and dy between the testing surface and the reference surface along the x and y directions, Eq. (4) can be obtained:

$$\begin{aligned} D_2 = D_2' + \text{residuals} &= a_{21}Z_1(x,y) + a_{22}Z_2(x,y) \\ &+ a_{23}Z_3(x,y) + a_{24}Z_4(x,y) - \sum_{i=5}^{k} a_i Z_i(x,y) \\ &+ \sum_{i=5}^{m} b_i Z_i'(x'+dx, y'+dy) + \text{residuals}. \end{aligned} \tag{4}$$

Considering that N measurements are taken in total, the goal of our proposed absolute measurement algorithm is to minimize the value of Eq. (5):

$$S = \sum_{i=1}^{N} (D_i - D_i')^2 = \min. \tag{5}$$

By calculating the partial derivative of Eq. (5) as described in Eq. (6), the function can be transformed into matrix form as shown in Eq. (7):

$$\begin{cases} \frac{\partial S}{\partial a_{i1}} = 0 \\ \frac{\partial S}{\partial a_{i2}} = 0 \\ \frac{\partial S}{\partial a_{i3}} = 0 \\ \frac{\partial S}{\partial a_{i4}} = 0 \\ \frac{\partial S}{\partial a_j} = 0 \\ \frac{\partial S}{\partial b_{j'}} = 0 \end{cases} \left(i = 1 \cdots N,\ j = 5 \cdots k,\ j' = 5 \cdots m\right), \tag{6}$$

$$P = Q \cdot R. \tag{7}$$

The final least-squares equation derived from Eq. (7) becomes

$$\begin{bmatrix} P_1 \\ P_2 \\ P_3 \\ \vdots \\ P_N \\ P_a \\ P_b \end{bmatrix} = \begin{bmatrix} Q_{11} & Q_{12} & Q_{13} & \cdots & Q_{1N} & Q_{1a} & Q_{1b} \\ Q_{21} & Q_{22} & Q_{23} & \cdots & Q_{2N} & Q_{2a} & Q_{2b} \\ Q_{31} & Q_{32} & Q_{33} & \cdots & Q_{3N} & Q_{3a} & Q_{3b} \\ \vdots & \vdots & \vdots & \ddots & \vdots & \vdots & \vdots \\ Q_{N1} & Q_{N2} & Q_{N3} & \cdots & Q_{NN} & Q_{Na} & Q_{Nb} \\ Q_{a1} & Q_{a2} & Q_{a3} & \cdots & Q_{aN} & Q_{aa} & Q_{ab} \\ Q_{b1} & Q_{b2} & Q_{b3} & \cdots & Q_{bN} & Q_{ba} & Q_{bb} \end{bmatrix} \begin{bmatrix} R_1 \\ R_2 \\ R_3 \\ \vdots \\ R_N \\ R_a \\ R_b \end{bmatrix}. \tag{8}$$

To better explain each term in Eq. (8), a detailed description of each element is shown in the following.

P is a $[(k+m-8)+4N]$ rows vector that can be described as

$$P_i = \begin{bmatrix} \sum_i D_i Z_1 \\ \sum_i D_i Z_2 \\ \sum_i D_i Z_3 \\ \sum_i D_i Z_4 \end{bmatrix} (i = 1 \cdots N) \quad P_a = \begin{bmatrix} \sum_{i=1}^{N} D_i Z_5 \\ \sum_{i=1}^{N} D_i Z_6 \\ \vdots \\ \sum_{i=1}^{N} D_i Z_k \end{bmatrix}$$

$$P_b = \begin{bmatrix} \sum_{i=1}^{N} D_i Z_5' \\ \sum_{i=1}^{N} D_i Z_6' \\ \vdots \\ \sum_{i=1}^{N} D_i Z_m' \end{bmatrix}. \tag{9}$$

Q is a matrix of size $[(k+m-8)+4N]$, and the elements in it can be expressed by Eqs. (10)–(16):

$$Q_{ii} = \begin{bmatrix} \sum_i Z_1^2 & \sum_i Z_1 Z_2 & \sum_i Z_1 Z_3 & \sum_i Z_1 Z_4 \\ \sum_i Z_2 Z_1 & \sum_i Z_2^2 & \sum_i Z_2 Z_3 & \sum_i Z_2 Z_4 \\ \sum_i Z_3 Z_1 & \sum_i Z_3 Z_2 & \sum_i Z_3^2 & \sum_i Z_3 Z_4 \\ \sum_i Z_4 Z_1 & \sum_i Z_4 Z_2 & \sum_i Z_4 Z_3 & \sum_i Z_4^2 \end{bmatrix} (i = 1, 2 \cdots N), \tag{10}$$

$$Q_{ij}=\begin{bmatrix}0&0&0&0\\0&0&0&0\\0&0&0&0\\0&0&0&0\end{bmatrix}\quad (i,\ j=1,2\cdots N,\ i\neq j), \tag{11}$$

$$Q_{ia}=Q_{ai}=\begin{bmatrix}\sum\limits_i Z_1Z_5 & \sum\limits_i Z_2Z_5 & \sum\limits_i Z_3Z_5 & \sum\limits_i Z_4Z_5\\ \sum\limits_i Z_1Z_6 & \sum\limits_i Z_2Z_6 & \sum\limits_i Z_3Z_6 & \sum\limits_i Z_4Z_6\\ \vdots & \vdots & \vdots & \vdots\\ \sum\limits_i Z_1Z_k & \sum\limits_i Z_2Z_k & \sum\limits_i Z_3Z_k & \sum\limits_i Z_4Z_k\end{bmatrix}$$

$$(i=1,2\cdots N), \tag{12}$$

$$Q_{ib}=Q_{bi}=\begin{bmatrix}\sum\limits_i Z_1Z'_5 & \sum\limits_i Z_2Z'_5 & \sum\limits_i Z_3Z'_5 & \sum\limits_i Z_4Z'_5\\ \sum\limits_i Z_1Z'_6 & \sum\limits_i Z_2Z'_6 & \sum\limits_i Z_3Z'_6 & \sum\limits_i Z_4Z'_6\\ \vdots & \vdots & \vdots & \vdots\\ \sum\limits_i Z_1Z'_m & \sum\limits_i Z_2Z'_m & \sum\limits_i Z_3Z'_m & \sum\limits_i Z_4Z'_m\end{bmatrix}$$

$$(i=1,2\cdots N), \tag{13}$$

$$Q_{bb}=\begin{bmatrix}\sum\limits_{i=1}^{N} Z'_5Z'_5 & \sum\limits_{i=1}^{N} Z'_5Z'_6 & \cdots & \sum\limits_{i=1}^{N} Z'_5Z'_m\\ \sum\limits_{i=1}^{N} Z'_6Z'_5 & \sum\limits_{i=1}^{N} Z'_6Z'_6 & \cdots & \sum\limits_{i=1}^{N} Z'_6Z'_m\\ \vdots & \vdots & \ddots & \vdots\\ \sum\limits_{i=1}^{N} Z'_mZ'_5 & \sum\limits_{i=1}^{N} Z'_mZ'_6 & \cdots & \sum\limits_{i=1}^{N} Z'_mZ'_m\end{bmatrix}, \tag{14}$$

$$Q_{aa}=\begin{bmatrix}\sum\limits_{i=1}^{N} Z_5Z_5 & \sum\limits_{i=1}^{N} Z_5Z_6 & \cdots & \sum\limits_{i=1}^{N} Z_5Z_k\\ \sum\limits_{i=1}^{N} Z_6Z_5 & \sum\limits_{i=1}^{N} Z_6Z_6 & \cdots & \sum\limits_{i=1}^{N} Z_6Z_k\\ \vdots & \vdots & \ddots & \vdots\\ \sum\limits_{i=1}^{N} Z_kZ_5 & \sum\limits_{i=1}^{N} Z_kZ_6 & \cdots & \sum\limits_{i=1}^{N} Z_kZ_k\end{bmatrix}, \tag{15}$$

$$Q_{ba}=Q_{ab}=\begin{bmatrix}\sum\limits_{i=1}^{N} Z'_5Z_5 & \sum\limits_{i=1}^{N} Z'_5Z_6 & \cdots & \sum\limits_{i=1}^{N} Z'_5Z_k\\ \sum\limits_{i=1}^{N} Z'_6Z_5 & \sum\limits_{i=1}^{N} Z'_6Z_6 & \cdots & \sum\limits_{i=1}^{N} Z'_6Z_k\\ \vdots & \vdots & \ddots & \vdots\\ \sum\limits_{i=1}^{N} Z'_mZ_5 & \sum\limits_{i=1}^{N} Z'_mZ_6 & \cdots & \sum\limits_{i=1}^{N} Z'_mZ_k\end{bmatrix}. \tag{16}$$

R is a $[(k+m-8)+4N]$ rows vector that can be written as

$$R_i=\begin{bmatrix}a_{1i}\\a_{2i}\\a_{3i}\\a_{4i}\end{bmatrix}\quad (i=1\cdots N)\quad R_a=\begin{bmatrix}a_5\\a_6\\\vdots\\a_k\end{bmatrix}\quad R_b=\begin{bmatrix}b_5\\b_6\\\vdots\\b_m\end{bmatrix}. \tag{17}$$

By combining Eqs. (8)–(17), the description of Eq. (7) can also be written as follows:

$$\begin{bmatrix}\sum\limits_1 D_1Z_1\\ \sum\limits_1 D_1Z_2\\ \sum\limits_1 D_1Z_3\\ \sum\limits_1 D_1Z_4\\ \sum\limits_2 D_2Z_1\\ \sum\limits_2 D_2Z_2\\ \sum\limits_2 D_2Z_3\\ \sum\limits_2 D_2Z_4\\ \vdots\\ \sum\limits_{i=1}^{N} D_iZ_5\\ \sum\limits_{i=1}^{N} D_iZ_6\\ \vdots\\ \sum\limits_{i=1}^{N} D_iZ_k\\ \sum\limits_{i=1}^{N} D_iZ'_5\\ \sum\limits_{i=1}^{N} D_iZ'_6\\ \vdots\\ \sum\limits_{i=1}^{N} D_iZ'_m\end{bmatrix}=\begin{bmatrix}\sum\limits_1 Z_1^2 & \sum\limits_1 Z_1Z_2 & \sum\limits_1 Z_1Z_3 & \sum\limits_1 Z_1Z_4 & 0 & 0 & 0 & 0 & \cdots & \sum\limits_1 Z_1Z_5 & \sum\limits_1 Z_1Z_6 & \cdots & \sum\limits_1 Z_1Z_k & \sum\limits_1 Z_1Z'_5 & \sum\limits_1 Z_1Z'_6 & \cdots & \sum\limits_1 Z_1Z'_m\\ \sum\limits_1 Z_2Z_1 & \sum\limits_1 Z_2^2 & \sum\limits_1 Z_2Z_3 & \sum\limits_1 Z_2Z_4 & 0 & 0 & 0 & 0 & \cdots & \sum\limits_1 Z_2Z_5 & \sum\limits_1 Z_2Z_6 & \cdots & \sum\limits_1 Z_2Z_k & \sum\limits_1 Z_2Z'_5 & \sum\limits_1 Z_2Z'_6 & \cdots & \sum\limits_1 Z_2Z'_m\\ \sum\limits_1 Z_3Z_1 & \sum\limits_1 Z_3Z_2 & \sum\limits_1 Z_3^2 & \sum\limits_1 Z_3Z_4 & 0 & 0 & 0 & 0 & \cdots & \sum\limits_1 Z_3Z_5 & \sum\limits_1 Z_3Z_6 & \cdots & \sum\limits_1 Z_3Z_k & \sum\limits_1 Z_3Z'_5 & \sum\limits_1 Z_3Z'_6 & \cdots & \sum\limits_1 Z_3Z'_m\\ \sum\limits_1 Z_4Z_1 & \sum\limits_1 Z_4Z_2 & \sum\limits_1 Z_4Z_3 & \sum\limits_1 Z_4^2 & 0 & 0 & 0 & 0 & \cdots & \sum\limits_1 Z_4Z_5 & \sum\limits_1 Z_4Z_6 & \cdots & \sum\limits_1 Z_4Z_k & \sum\limits_1 Z_4Z'_5 & \sum\limits_1 Z_4Z'_6 & \cdots & \sum\limits_1 Z_4Z'_m\\ 0 & 0 & 0 & 0 & \sum\limits_2 Z_1^2 & \sum\limits_2 Z_1Z_2 & \sum\limits_2 Z_1Z_3 & \sum\limits_2 Z_1Z_4 & \cdots & \sum\limits_2 Z_1Z_5 & \sum\limits_1 Z_1Z_6 & \cdots & \sum\limits_2 Z_1Z_k & \sum\limits_2 Z_1Z'_5 & \sum\limits_2 Z_1Z'_6 & \cdots & \sum\limits_2 Z_1Z'_m\\ 0 & 0 & 0 & 0 & \sum\limits_2 Z_2Z_1 & \sum\limits_2 Z_2^2 & \sum\limits_2 Z_2Z_3 & \sum\limits_2 Z_2Z_4 & \cdots & \sum\limits_2 Z_2Z_5 & \sum\limits_2 Z_2Z_6 & \cdots & \sum\limits_2 Z_2Z_k & \sum\limits_2 Z_2Z'_5 & \sum\limits_2 Z_2Z'_6 & \cdots & \sum\limits_2 Z_2Z'_m\\ 0 & 0 & 0 & 0 & \sum\limits_2 Z_3Z_1 & \sum\limits_2 Z_3Z_2 & \sum\limits_2 Z_3^2 & \sum\limits_2 Z_3Z_4 & \cdots & \sum\limits_2 Z_3Z_5 & \sum\limits_1 Z_3Z_6 & \cdots & \sum\limits_2 Z_3Z_k & \sum\limits_2 Z_3Z'_5 & \sum\limits_2 Z_3Z'_6 & \cdots & \sum\limits_2 Z_3Z'_m\\ 0 & 0 & 0 & 0 & \sum\limits_2 Z_4Z_1 & \sum\limits_2 Z_4Z_2 & \sum\limits_2 Z_4Z_2 & \sum\limits_2 Z_4^2 & \cdots & \sum\limits_2 Z_4Z_5 & \sum\limits_1 Z_4Z_6 & \cdots & \sum\limits_2 Z_4Z_k & \sum\limits_2 Z_4Z'_5 & \sum\limits_2 Z_4Z'_6 & \cdots & \sum\limits_2 Z_4Z'_m\\ \vdots & \vdots & \vdots & \vdots & \vdots & \vdots & \vdots & \vdots & \ddots & \vdots & \vdots & \ddots & \vdots & \vdots & \vdots & \ddots & \vdots\\ \sum\limits_1 Z_1Z_5 & \sum\limits_1 Z_2Z_5 & \sum\limits_1 Z_3Z_5 & \sum\limits_1 Z_4Z_5 & \sum\limits_2 Z_1Z_5 & \sum\limits_2 Z_2Z_5 & \sum\limits_2 Z_3Z_5 & \sum\limits_2 Z_4Z_5 & \cdots & \sum\limits_{i=1}^{N} Z_5Z_5 & \sum\limits_{i=1}^{N} Z_5Z_6 & \cdots & \sum\limits_{i=1}^{N} Z_5Z_k & \sum\limits_{i=1}^{N} Z_5Z'_5 & \sum\limits_{i=1}^{N} Z_5Z'_6 & \cdots & \sum\limits_{i=1}^{N} Z_5Z'_m\\ \sum\limits_1 Z_1Z_6 & \sum\limits_1 Z_2Z_6 & \sum\limits_1 Z_3Z_6 & \sum\limits_1 Z_4Z_6 & \sum\limits_1 Z_1Z_6 & \sum\limits_1 Z_2Z_6 & \sum\limits_1 Z_3Z_6 & \sum\limits_1 Z_4Z_6 & \cdots & \sum\limits_{i=1}^{N} Z_6Z_5 & \sum\limits_{i=1}^{N} Z_6Z_6 & \cdots & \sum\limits_{i=1}^{N} Z_6Z_k & \sum\limits_{i=1}^{N} Z_6Z'_5 & \sum\limits_{i=1}^{N} Z_6Z'_6 & \cdots & \sum\limits_{i=1}^{N} Z_6Z'_m\\ \vdots & \vdots & \vdots & \vdots & \vdots & \vdots & \vdots & \vdots & \ddots & \vdots & \vdots & \ddots & \vdots & \vdots & \vdots & \ddots & \vdots\\ \sum\limits_1 Z_1Z_k & \sum\limits_1 Z_2Z_k & \sum\limits_1 Z_3Z_k & \sum\limits_1 Z_4Z_k & \sum\limits_2 Z_1Z_k & \sum\limits_2 Z_2Z_k & \sum\limits_2 Z_3Z_k & \sum\limits_2 Z_4Z_k & \cdots & \sum\limits_{i=1}^{N} Z_kZ_5 & \sum\limits_{i=1}^{N} Z_kZ_6 & \cdots & \sum\limits_{i=1}^{N} Z_kZ_k & \sum\limits_{i=1}^{N} Z_kZ'_5 & \sum\limits_{i=1}^{N} Z_kZ'_6 & \cdots & \sum\limits_{i=1}^{N} Z_kZ'_m\\ \sum\limits_1 Z_1Z'_5 & \sum\limits_1 Z_2Z'_5 & \sum\limits_1 Z_3Z'_5 & \sum\limits_1 Z_4Z'_5 & \sum\limits_2 Z_1Z'_5 & \sum\limits_2 Z_2Z'_5 & \sum\limits_2 Z_3Z'_5 & \sum\limits_2 Z_4Z'_5 & \cdots & \sum\limits_{i=1}^{N} Z'_5Z_5 & \sum\limits_{i=1}^{N} Z'_5Z_6 & \cdots & \sum\limits_{i=1}^{N} Z'_5Z_k & \sum\limits_{i=1}^{N} Z'_5Z'_5 & \sum\limits_{i=1}^{N} Z'_5Z'_6 & \cdots & \sum\limits_{i=1}^{N} Z'_5Z'_m\\ \sum\limits_1 Z_1Z'_6 & \sum\limits_1 Z_2Z'_6 & \sum\limits_1 Z_3Z'_6 & \sum\limits_1 Z_4Z'_6 & \sum\limits_2 Z_1Z'_6 & \sum\limits_2 Z_2Z'_6 & \sum\limits_2 Z_3Z'_6 & \sum\limits_2 Z_4Z'_6 & \cdots & \sum\limits_{i=1}^{N} Z'_6Z_5 & \sum\limits_{i=1}^{N} Z'_6Z_6 & \cdots & \sum\limits_{i=1}^{N} Z'_6Z_k & \sum\limits_{i=1}^{N} Z'_6Z'_5 & \sum\limits_{i=1}^{N} Z'_6Z'_6 & \cdots & \sum\limits_{i=1}^{N} Z'_6Z'_m\\ \vdots & \vdots & \vdots & \vdots & \vdots & \vdots & \vdots & \vdots & \ddots & \vdots & \vdots & \ddots & \vdots & \vdots & \vdots & \ddots & \vdots\\ \sum\limits_1 Z_1Z'_m & \sum\limits_1 Z_2Z'_m & \sum\limits_1 Z_3Z'_m & \sum\limits_1 Z_4Z'_m & \sum\limits_2 Z_1Z'_m & \sum\limits_2 Z_2Z'_m & \sum\limits_2 Z_3Z'_m & \sum\limits_2 Z_4Z'_m & \cdots & \sum\limits_{i=1}^{N} Z'_mZ_5 & \sum\limits_{i=1}^{N} Z'_mZ_6 & \cdots & \sum\limits_{i=1}^{N} Z'_mZ_k & \sum\limits_{i=1}^{N} Z'_mZ'_5 & \sum\limits_{i=1}^{N} Z'_mZ'_6 & \cdots & \sum\limits_{i=1}^{N} Z'_mZ'_m\end{bmatrix}\begin{bmatrix}a_{11}\\a_{12}\\a_{13}\\a_{14}\\a_{21}\\a_{22}\\a_{23}\\a_{24}\\\vdots\\a_5\\a_6\\\vdots\\a_k\\b_5\\b_6\\\vdots\\b_m\end{bmatrix}. \tag{18}$$

The coefficients of Zernike terms $a_5 \sim a_k$ and $b_5 \sim b_m$ can be calculated from Eq. (18) with the QR decomposition method, which also means N subaperture testing maps are stitched together with the above algorithm. Our stitching algorithm can be expressed with Eqs. (5)–(18). However, the powers of both the reference surface and the test surface cannot be solved with the above method. In fact, they can be calculated by other methods such as pentaprism scanning [21]. The pentaprism scanning testing method is an important absolute test method for flat mirrors. During a measurement, a pentaprism is used to relay a collimated beam from an autocollimator to the surface under test. The pentaprism scans in a line along the surface to obtain a series of slope measurements. Multiple scans can be combined together to get aberration information of the surface under test [22]. By calculating the Zernike fitting coefficients, maps of both the reference surface and the test surface can be obtained.

3. SIMULATION

In this part, in order to validate the accuracy and feasibility of our proposed absolute measurement method, simulation is taken to reconstruct both the test surface and the reference surface. In the simulation, a Φ150 mm diameter reference surface is used to test a Φ150 mm test surface. The surface errors of them are shown in Fig. 1.

The root mean square (RMS) of the test surface is 9.59 nm, and the RMS of the reference surface is 9.64 nm. In the testing, nine measurements are designed as shown in Fig. 2. The central subaperture coincides with the position of the mirror to be measured. The relation between the second and the ninth subapertures and the position of the mirror to be measured is (0, 15), (0, −15), (15, 0), (−15, 0), (10, 10), (10, −10), (−10, −10), and (−10, 10) in the x and y directions, respectively (the unit in the above translation is mm). Relative translations are taken between the test surface and the reference surface in each measurement.

In the simulation, alignment errors in the x and y directions, tip/tilt errors, piston errors between the reference surface and the test surface, and noise of 1 nm RMS are considered in each measurement. A total of 79 terms of Zernike polynomials that can accurately describe the surface features are used to fit both the test surface and the reference surface. Usually 37 terms of Zernike polynomials are used to fit the wavefront estimation in most applications. In fact, the RMS value deviation percentage between 37-term and 79-term Zernike polynomials in our simulation is about 0.002. To better describe the simulation result, 79 terms of Zernike polynomials are chosen.

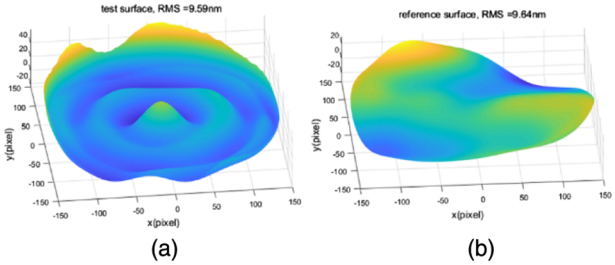

Fig. 1. Original surfaces. (a) Original test surface. (b) Original reference surface.

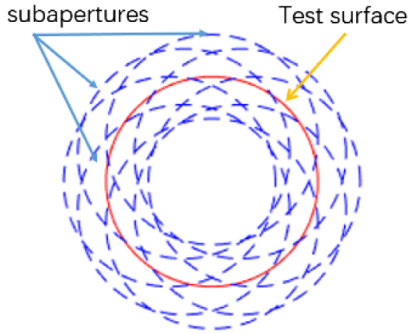

Fig. 2. Relative positions between reference surface and test surface in measurements.

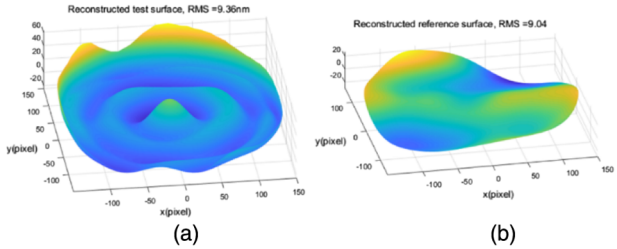

Fig. 3. Reconstructed surfaces. (a) Reconstructed test surface. (b) Reconstructed reference surface.

Combining the theory introduced in Section 2, the subaperture number is 9, which means N is equal to 9 in Eq. (8). A total of 79 terms of Zernike polynomials are chosen to describe the surface features of both the test surface and the reference surface, which means that both k and m are equal to 79 in Eq. (9). Then P is a $(186 * 1)$ vector in Eqs. (8) and (9). Q is a $(186 * 186)$ matrix, and R is a $(186 * 1)$ vector in Eqs. (8) and (9). With our proposed absolute measurement method, the reconstruction maps of the test and reference surfaces are shown in Fig. 3.

The RMS of the reconstructed test surface is 9.36 nm, and the RMS of the reconstructed reference surface is 9.04 nm. It can be seen from Figs. 2 and 3 that the original surfaces are consistent with the reconstructed surfaces. In order to better explain the reconstruction accuracy, residual maps between original surfaces and reconstructed surfaces are analyzed as shown in Fig. 4.

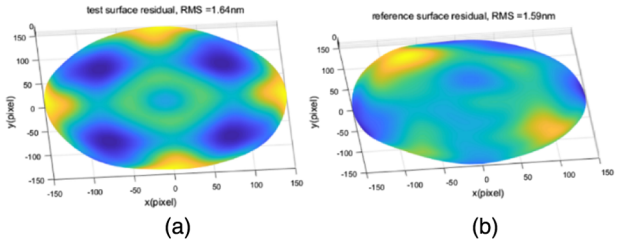

Fig. 4. Surfaces residuals. (a) Residual of test surface. (b) Residual of reference surface.

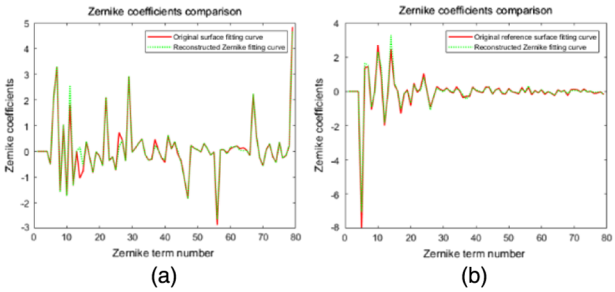

Fig. 5. (a) Zernike coefficient comparison between original testing surface and reconstructed testing surface. (b) Zernike coefficient comparison between original reference surface and reconstructed reference surface.

The RMS of the test surface residual is 1.64 nm, and the RMS of the reference surface is 1.59 nm. It can be seen from Fig. 4 that the residuals are very small and that they are at the same level as the noise error. The Zernike polynomial coefficients are also analyzed as shown in Fig. 5. In Fig. 5(a), the Zernike coefficients of the test surface are compared between the original test surface and the reconstructed test surface. In Fig. 5(b), the Zernike coefficients of the reference surface between the original reference surface and the reconstructed reference surface are also compared. From the fitting curves, it can be seen that the original Zernike fitting curves are consistent with Zernike fitting curves of reconstructed surfaces. This means that our proposed absolute measurement method can reconstruct both the reference surface and the test surface with satisfactory accuracy.

4. EXPERIMENT VERIFICATION

We have also applied our absolute measurement method on a real experiment to further validate the practicability of the proposed method. In the experiment, a Φ150 mm Zygo interferometer is applied to test the other Φ150 mm Zygo standard surface. The optical metrology layout is shown in Fig. 6, and the experimental setup is shown in Fig. 7. The registration issue between testing subapertures is handled with a 6-dof platform, which includes the X, Y, Z, A, B, and C axes. The relative relationship between each axis is shown in Fig. 8. The range of movement and relative accuracy of each axis can be found in Table 1.

Nine measurements are taken following the relative positions between the test surface and the reference surface as shown in Fig. 2. The relative testing maps are shown in Fig. 9. In addition, a total of 79 terms of Zernike polynomials that can accurately describe the surface features are used to fit both the test surface

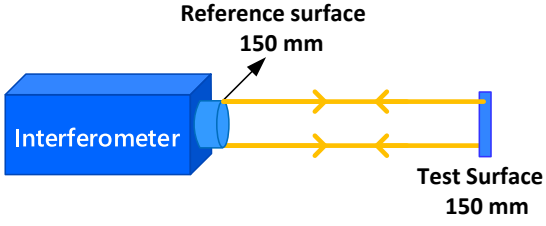

Fig. 6. Optical metrology layout.

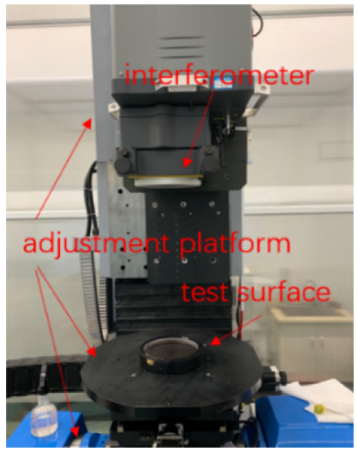

Fig. 7. Experimental setup.

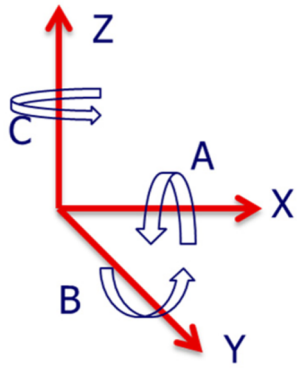

Fig. 8. Description of 6-dof platform.

Table 1. Range and Accuracy of 6-dof Platform

Axis	Range of Movement	Accuracy
X	1000 mm	0.01 mm
Y	500 mm	0.01 mm
Z	800 mm	0.02 mm
A	90°	4″
B	3°	4″
C	360°	10″

and the reference surface. With our proposed absolute measurement method, both the test surface and the reference surface are reconstructed as shown in Fig. 10. The RMS of the test surface is 12.73 nm, and the RMS of the reference surface is 6.36 nm. By removing the reconstructed reference surface and the test surface from the central measurement result shown in Fig. 8, the relative residual map is shown in Fig. 11. The RMS of the residual map is 1.24 nm. It can be seen from Fig. 11 that the high-frequency errors are the main components of the residual map. In actual testing, there is 0.046λ power, which cannot be decomposed into reference and test surfaces. The power of the test surface should be tested and added in our above reconstructed map in the end.

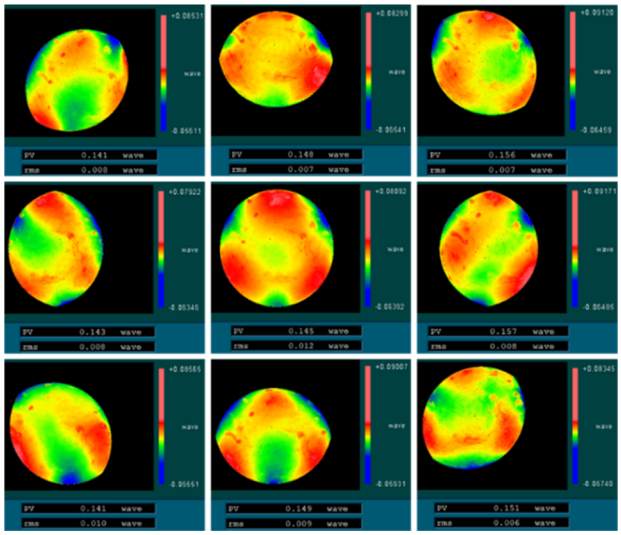

Fig. 9. Measurement maps.

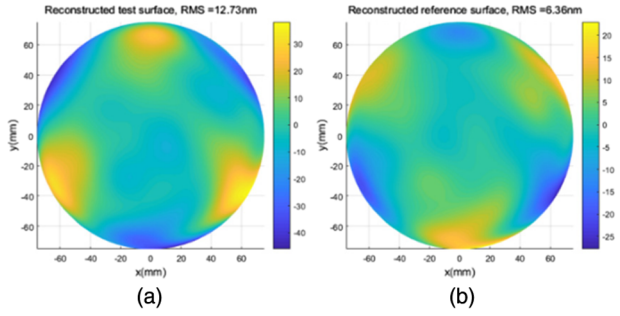

Fig. 10. Reconstructed surfaces. (a) Reconstructed test surface. (b) Reconstructed reference surface.

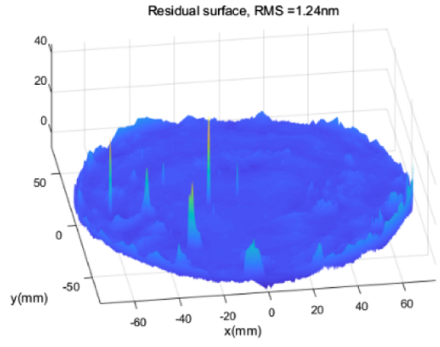

Fig. 11. Residual map.

5. CONCLUSION

In this paper, we have proposed an absolute measurement method based on Zernike polynomial fitting. Both the reference surface and the test surface can be reconstructed at the same time. Our simulation results and experimental results have demonstrated that our proposed method can correctly reconstruct absolute surfaces with satisfactory accuracy. Since no rotation between the test surface and the reference surface is conducted during testing, part of the surface errors cannot be extracted. We will further study the relationship between the residual error extraction and the relative rotation in future research.

Funding. the Fundamental Research Funds for Key Laboratory of Opto-electronic Information Acquisition and Manipulation of Ministry of Education (OEIAM202009); Fundamental Research Funds for the Central Universities (2018KFYYXJJ053, 2019kfyRCPY083, 2019kfyXKJC040); National Natural Science Foundation of China (61805088, 61805089).

Disclosures. The authors declare no conflicts of interest.

REFERENCES

1. R. Bünnagel, H. A. Oehring, and K. Steiner, "Fizeau interferometer for measuring the flatness of optical surfaces," Appl. Opt. **7**, 331–335 (1968).
2. M. Vannoni and G. Molesini, "Validation of absolute planarity reference plates with a liquid mirror," Metrologia **42**, 389–393 (2005).
3. G. Schulz and J. Schwider, "Precise measurement of planeness," Appl. Opt. **6**, 1077–1084 (1967).
4. B. S. Fritz, "Absolute calibration of an optical flat," Opt. Eng. **23**, 379–383 (1984).
5. U. Griesmann, "Three-flat test solutions based on simple mirror symmetry," Appl. Opt. **45**, 5856–5865 (2006).
6. C. Xu, L. Chen, and J. Yin, "Method for absolute flatness measurement of optical surfaces," Appl. Opt. **48**, 2536–2541 (2009).
7. H. Y. Quan, X. Hou, F. Wu, and W. H. Song, "Absolute measurement of optical flats based on basic iterative methods," Opt. Express **23**, 16305–16319 (2015).
8. Z. Han, L. Chen, T. Wulan, and R. Zhu, "The absolute flatness measurements of two aluminum coated mirrors based on the skip flat test," Optik **124**, 3781–3785 (2013).
9. L. B. Xu, S. J. Liu, R. H. Zhu, Y. Zhou, and J. Chen, "Absolute surface form measurement of flat optics based on oblique incidence method," Chin. Opt. Lett. **16**, 101201 (2018).
10. P. B. Keenan, "Pseudo-shear interferometry," Proc. SPIE **123**, 2–9 (1984).
11. E. E. Bloemhof, "Absolute surface metrology with a phase-shifting interferometer for incommensurate transverse spatial shifts," Appl. Opt. **53**, 792–797 (2014).
12. J. Ma, C. Pruss, R. Zhu, Z. Gao, C. Yuan, and Y. Wan, "An absolute test for axicon surfaces," Opt. Lett. **36**, 2005–2007 (2011).
13. Y. Huang, J. Ma, R. H. Zhu, C. J. Yuan, L. Cen, H. J. Cai, and W. Y. Sun, "Absolute measurement of optical flat surface shape based on the conjugate differential method," Opt. Express **23**, 29687–29697 (2015).
14. P. Su, J. H. Burge, and R. E. Parks, "Application of maximum likelihood reconstruction of subaperture data for measurement of large flat mirrors," Appl. Opt. **49**, 21–31 (2010).
15. D. Q. Su, E. L. Miao, Y. X. Sui, and H. J. Yang, "Absolute surface figure testing by shift-rotation method using Zernike polynomials," Opt. Lett. **37**, 3198–3200 (2012).
16. L. S. Yan, W. Luo, G. J. Yan, X. K. Wang, H. D. Zhang, L. Y. Chao, D. L. Ma, and X. H. Tang, "Subaperture stitching testing for fine flat mirrors with large apertures using an orthonormal polynomial fitting algorithm," Opt. Laser Eng. **120**, 49–58 (2019).
17. Z. M. Yang, Z. S. Gao, D. Zhu, and Q. Yuan, "Absolute ultra-precision measurement of high-numerical-aperture spherical surface by high-order shift-rotation method using Zernike polynomials," Opt. Commun. **355**, 191–199 (2015).
18. Z. M. Yang, J. Y. Du, C. Tian, J. T. Dou, Q. Yuan, and Z. S. Gao, "Generalized shift-rotation absolute measurement method for high-numerical-aperture spherical surfaces with global optimized wavefront reconstruction algorithm," Opt. Express **25**, 26133–26147 (2017).

19. N. M. Virendra and G. M. Dai, "Orthonormal polynomials in wavefront analysis: analytical solution," J. Opt. Soc. Am. A **24**, 2294–3016 (2007).
20. G. M. Dai and N. M. Virendra, "Nonrecursive determination of orthonormal polynomials with matrix formulation," Opt. Lett. **32**, 74–76 (2007).
21. J. Yellowhair and J. H. Burge, "Analysis of a scanning pentaprism system for measurements of large flat mirrors," Appl. Opt. **46**, 8466–8474 (2007).
22. P. Su, "Absolute measurements of large mirrors," Ph.D. thesis (University of Arizona, 2008).